Available online at www.sciencedirect.com
ScienceDirect
Magnetic Resonance Imaging 26 (2008) 1041 – 1054
MAGNETIC RESONANCE IMAGING

Across-trial averaging of event-related EEG responses and beyond

A. Mouraux[a], G.D. Iannetti[b,*]

[a]Oxford Centre for Functional Magnetic Resonance Imaging of the Brain (FMRIB), Oxford, United Kingdom
[b]Department of Physiology, Anatomy and Genetics, University of Oxford, Oxford, United Kingdom

Received 17 December 2007; accepted 14 January 2008

Abstract

Internally and externally triggered sensory, motor and cognitive events elicit a number of transient changes in the ongoing electroencephalogram (EEG): event-related brain potentials (ERPs), event-related synchronization and desynchronization (ERS/ERD), and event-related phase resetting (ERPR). To increase the signal-to-noise ratio of event-related brain responses, most studies rely on across-trial averaging in the time domain, a procedure that is, however, blind to a significant fraction of the elicited cortical activity. Here, we outline the key concepts underlying the limitations of time-domain averaging and consider three alternative methodological approaches that have received increasing interest: time-frequency decomposition of the EEG (using the continuous wavelet transform), blind source separation of the EEG (using Independent Component Analysis) and the analysis of event-related brain responses at the level of single trials. In addition, we provide practical guidelines on the implementation of these methods and on the interpretation of the results they produce.

Keywords: EEG analysis; Electrophysiology; Event-related potentials (ERPs); Event-related desynchronization (ERD); Event-related synchronization (ERS); Event-related phase resetting (ERPR); Time-frequency analysis; Blind source separation (BSS); Independent component analysis (ICA); Single-trial analysis

1. Electrical brain responses to transient events

The ongoing electrical activity of the human brain can be directly sampled through the skull, using one or an array of electrodes placed on the scalp. The recorded electrical activity (the electroencephalogram, EEG) mainly reflects summated, slow post-synaptic potentials of cortical neurons [1]. Sensory, motor or cognitive events (such as a fast-rising sensory stimulus, a brisk self-paced movement or a stimulus-triggered cognitive task) can elicit transient changes in this ongoing electrical activity [2]. However, only a fraction of these changes actually translates into responses that are measurable in the scalp EEG, because the elicited neuronal activity must satisfy a number of conditions to become detectable:

(1) The elicited neuronal activity must generate a relatively strong electrical field, and, therefore, it must involve a large population of neurons.
(2) The neural activity must be synchronous. Indeed, if the activity is temporally dispersed, the resulting electrical field will be diluted over time, and the signal difficult to measure on the scalp.
(3) The activated neuronal population must constitute an open field structure. If its geometrical configuration constitutes a closed field structure (e.g., neurons of a subcortical nucleus, organized in a radially symmetric configuration), the net electrical field outside the active structure will be null, as the electrical fields produced by the neurons of that structure will cancel each other.
(4) The time course of the elicited electrical activity must be relatively slow changing, as the skull and scalp interface act as a low-pass filter [3]. Therefore, scalp EEG does not include much of the high-frequency activity evident, for example, in direct intracortical recordings.

1.1. Event-related potentials

It is generally accepted that event-related potentials (ERPs) reflect synchronous changes of slow postsynaptic

* Corresponding author.
E-mail address: iannetti@fmrib.ox.ac.uk (G.D. Iannetti).

0730-725X/$ – see front matter © 2008 Elsevier Inc. All rights reserved.
doi:10.1016/j.mri.2008.01.011

potential occurring within a large number of similarly oriented cortical pyramidal neurons of a compact area of the cortex [1].[1] ERPs consist in brief monophasic deflections embedded in the background EEG. These deflections are characterized by their polarity, peak latency (relative to the onset of the event), peak amplitude (relative to a baseline) and scalp distribution.[2]

1.2. Event-related synchronization and desynchronization

It is known since the first EEG recordings described by Hans Berger in 1929 [5] that, in addition to triggering ERPs, various events may also trigger transient power modulations of the ongoing EEG oscillatory activity. These modulations may appear either as a transient increase (event-related synchronization, ERS) or as a transient decrease (event-related desynchronization, ERD) of power, usually confined within a specific frequency band of the EEG. The terms 'synchronization' and 'desynchronization' reflect the view that the increase/reduction in EEG oscillation power results from a synchronization/desynchronization of the activity of a population of neurons, and not from an overall increase/decrease of single-neuron activity. It is important to highlight that the functional significance of ERD and ERS differs according to the affected frequency band. ERS in the alpha frequency band (8–12 Hz) is often hypothesized to reflect cortical deactivation or inhibition, while ERD in the same frequency band is hypothesized to reflect cortical activation or disinhibition [6]. These hypotheses rely on experimental results showing, for example, that the power of alpha band rhythms is enhanced over the hand area during visual processing, or during foot movements [7]. In contrast, ERS in the gamma frequency band (25–100 Hz) is thought to subtend the formation of transient functional neuronal assemblies, possibly over large distances [8]. Gamma-band ERS could therefore play an important role for synchronizing cortical processes occurring within and possibly between different brain areas, a mechanism to integrate different features of sensory inputs into a coherent and meaningful percept [9]. In addition to the frequency (or range of frequencies) affected, ERS and ERD are characterized by their latency relative to event onset, their magnitude relative to a baseline level, and their scalp distribution.

1.3. Event-related phase resetting

In addition to ERPs, ERS and ERD, a number of investigators [10] have suggested that various events may also trigger a transient reorganization (or 'resetting') of the phase of ongoing EEG oscillations (event-related phase resetting, ERPR), although the physiological plausibility of this phenomenon remains to be demonstrated [10]. Phase resetting is common to nonlinear oscillatory systems in response to a perturbation and has been observed in a number of biological systems such as circadian rhythms and the electrocardiogram [11].

2. Detecting electrical EEG brain responses to transient events: time-domain averaging

The magnitude of event-related EEG responses is often several factors smaller than the magnitude of the background ongoing EEG. Therefore, the identification and characterization of these event-related brain responses rely on signal-processing methods of enhancing their signal-to-noise ratio. All these methods require repeating the event of interest a given number of times. The scalp EEG recording is then segmented into epochs, centred around each single event, and all epochs are averaged into a single waveform (time-domain averaging) [12,13]. The obtained waveform expresses the average scalp potential as a function of time relative to the onset of the event. The basic assumption underlying this procedure is that ERPs are *stationary* (i.e., their latency and morphology are invariant) and will therefore be unaffected by the averaging procedure. On the contrary, ongoing electrical brain activity behaves as noise unrelated to the event, and will therefore be largely cancelled out. Consequently, time-domain averaging will enhance the signal-to-noise ratio of stationary ERPs (Figs. 1 and 2).

Although useful in many instances, there are several issues related to time-domain averaging. In the following section, we will show (i) how time-domain averaging may distort or even miss ERPs that are not perfectly time-locked to the onset of the stimulus, (ii) how it is completely blind to ERS and ERD, and (iii) how it may mistakenly identify ERPRs as ERPs. Finally, we will show that it is often difficult to disentangle the different brain processes that may contribute to the signal recorded on the scalp.

2.1. ERPs affected by latency jitter

A critical assumption underlying time-domain averaging is that ERPs are stationary across trials. In some circumstances, this assumption is reasonable, for example when considering the early brain responses elicited by the direct electrical activation of a peripheral nerve (a stimulation producing a highly reproducible and synchronous afferent volley). However, there are many instances in which the different processes that separate the occurrence of the event from the generation of the cortical response result in a significant increase of the across-trial variability of response

[1] Recent evidence has also suggested that high-frequency components (600 Hz) of the EEG response elicited by the electrical stimulation of the median nerve may be a direct correlate of spike discharges in cortical neurons [4].

[2] The scalp distribution of the deflection can also be used to infer the location of their underlying neural sources, using models of how neural activity translates into scalp potentials. However, because an infinite number of source configurations can explain any given distribution of scalp potentials, additional assumptions (e.g., number of contributing sources, anatomical constraints on their locations) must be made, therefore limiting the trustworthiness of these approaches.

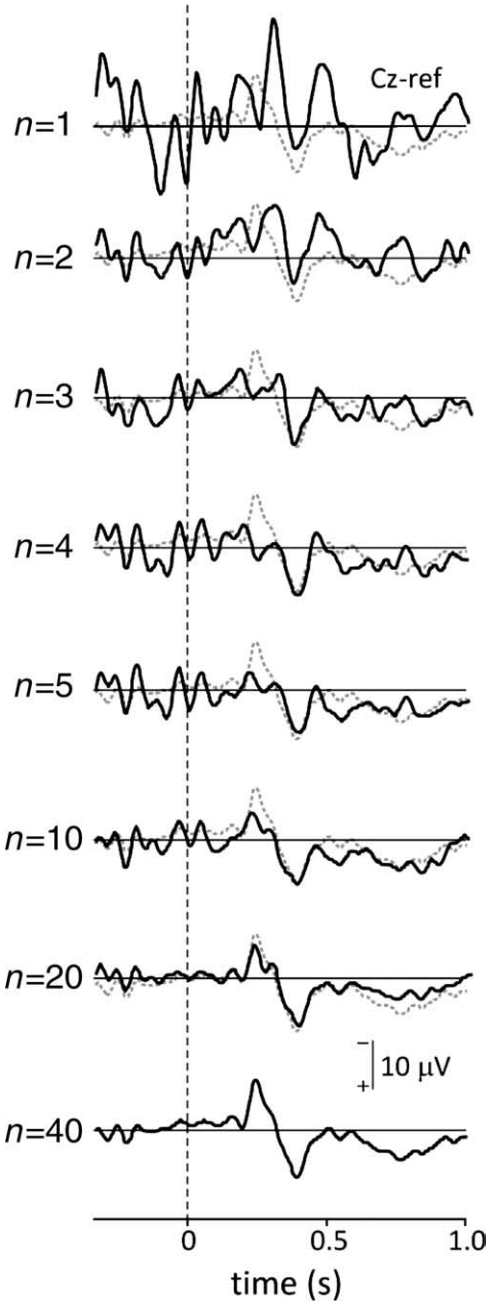

Fig. 1. Increase of signal-to-noise ratio by across-trial averaging of EEG epochs in the time domain. Event-related brain responses were elicited by brief infrared laser pulses (activating Aδ-fibre skin nociceptors) applied to the dorsum of the right hand and recorded from the vertex (Cz-nose reference). The black waveform on the top row represents the EEG response to the first stimulus. The black waveforms in the following rows represent the average of an increasing number of trials (defined by *n*). For comparison, the average of 40 trials is superimposed as a dotted waveform. Note how the signal-to-noise ratio improves by averaging a progressively greater number of trials.

latency: brain responses reflecting high-level cognitive processes, brain responses elicited by the stimulation of afferent nerve fibres having slow and variable conduction velocities (such as small-myelinated Aδ and unmyelinated C fibres), brain responses elicited by the natural stimulation of skin receptors (because of the additional transduction processes required to convert the energy of the stimulus into electrical impulses).

In these instances, the significant latency jitter may lead to an important distortion of the averaged ERP. At best, this distortion will result in an underestimation of the ERP peak amplitude, whose average will be spread over time (Figs. 2 and 3). At worst, it will render the ERP undetectable. An important implication of this is that a difference in amplitude of an average ERP recorded in two experimental conditions can result from a difference in latency jitter between conditions [14]. In addition, if the distribution of latency jitter is skewed (e.g., a Poisson distribution), the difference in latency jitter between conditions will also be reflected by a difference in the peak latency of the average ERP (Fig. 3).

The extent to which latency jitter affects ERPs averaged in the time domain varies as a function of the duration of the scalp deflection. Indeed, in the presence of the same latency jitter, a long-lasting deflection will be more stationary than a short-lasting deflection and, consequently, less distorted by time-domain averaging. Because it is reasonable to assume that the longer the latency of a given brain response, the greater its latency jitter, this could explain why short-lasting ERPs are only found at early latencies, and why late-latency ERPs are always long-lasting responses. Therefore, it could well be that transient events elicit a large number of late-latency, short-lasting ERPs, but that these remain undetected because a significant latency jitter distorts them beyond recognition.

2.1.1. ERD and ERS

Because ongoing EEG oscillations are unrelated to the stimulus, their phase is not stationary across trials (i.e., relative to the onset of the stimulus, their phases are homogeneously distributed across trials). Therefore, as the signal changes related to these 'non-phase-locked' oscillations behave like uncorrelated noise, they are largely cancelled out by time-domain averaging (Fig. 2). For this reason, time-domain averaging is unable to reveal any event-related transient modulation of power, despite being time locked to the stimulus onset.

2.1.2. ERPs and ERPRs

In recent years, attention has been drawn to the fact that electrical brain responses appearing as ERPs in the time-domain average waveform could, at least in some cases, be explained by an event-related resetting of the phase of the ongoing EEG (event-related phase resetting, ERPR). If, at a given latency, an event resets the phase of ongoing EEG oscillations, they will become transiently phase-locked to the onset of the event and, therefore, become transiently visible after time-domain averaging. As ERPR may produce a deflection entirely similar to that produced by an ERP (Fig. 2), time- domain averaging is unable to distinguish between the two types of electrical brain responses.

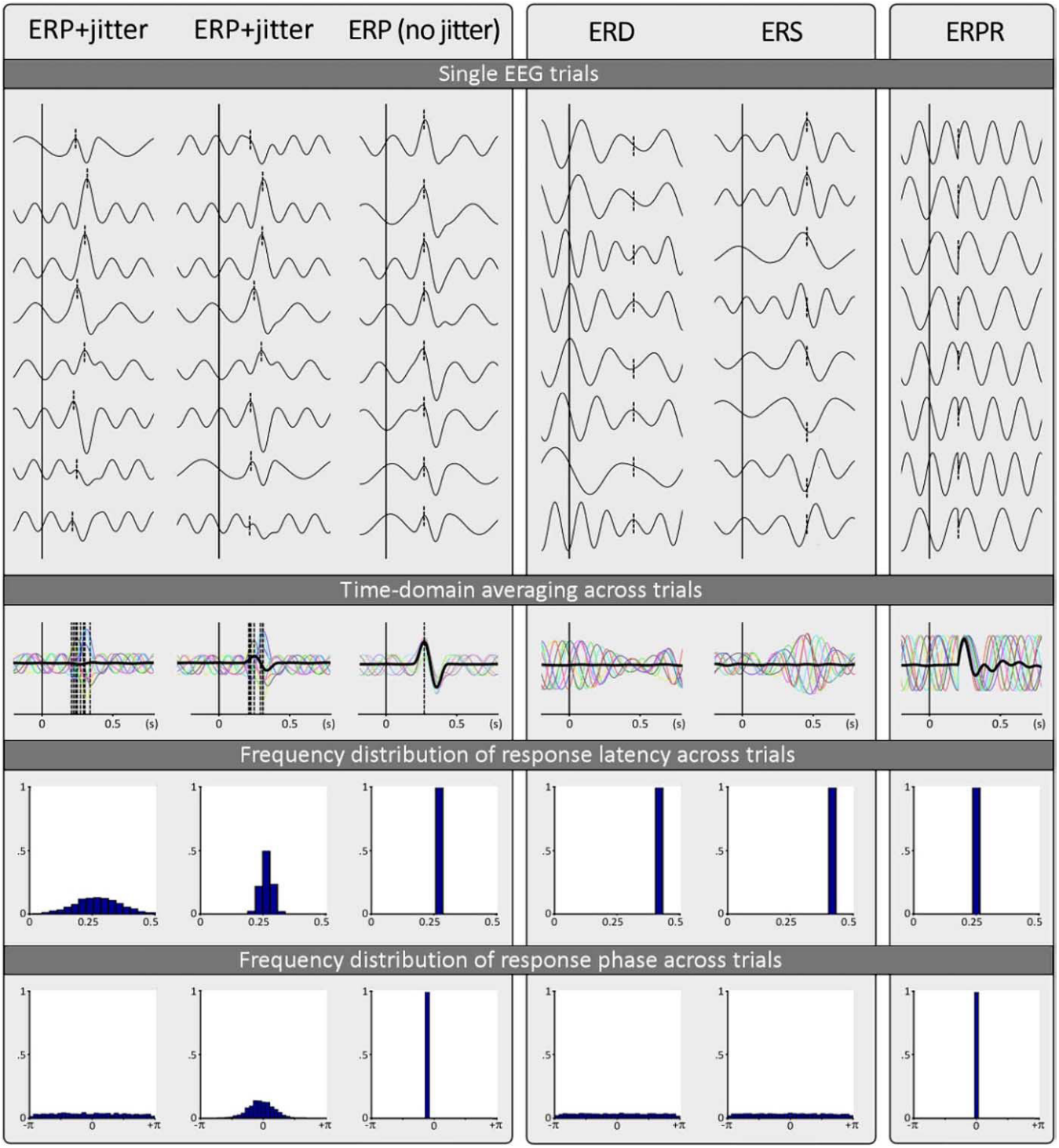

Fig. 2. Effect of across-trial averaging in the time domain on different models of event-related EEG brain responses. Event-related potentials (ERPs) were modelled as a time-locked deflection embedded in background oscillatory activity. In the left panel (ERP), the latency of the response was either varied from trial to trial using a significant jitter (left waveforms) or a moderate jitter (middle waveforms), or constant across trials (right waveforms). In the middle panel (ERD and ERS), ERD and ERS were modelled as time-locked decreases or increases of the amplitude of ongoing, non-phase-locked oscillations. In the right panel (ERPR), event-related phase resetting (ERPR) was modelled as a time-locked resetting of the phase of ongoing, initially non-phase-locked oscillations. A sample of non-averaged, single-trial waveforms is shown in the upper part of the figure, with the latency of the event-related activity represented as a dashed vertical line. The result of across-trial time-domain averaging is shown in the middle part of the figure, superimposed to the single-trial waveforms (represented in color). Note how the procedure (1) enhances the signal-to-noise ratio of ERPs when no jitter is present, but (2) produces a distorted average ERP when latency jitter is present, (3) completely cancels out the non-phase-locked oscillations underlying ERD and ERS, and (4) represents ERPR as a transient deflection that could be mistaken for an ERP. The histograms in the bottom part of the figure represent the frequency distributions of response latency and response phase across trials. (For interpretation of the references to color in this figure legend, the reader is referred to the web version of this article.)

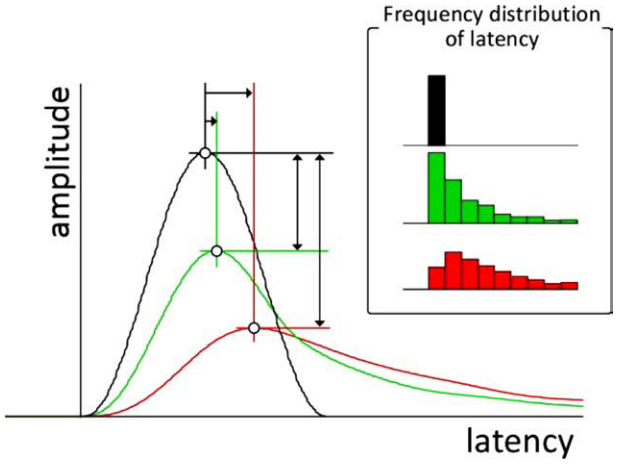

Fig. 3. Effect of latency jitter on the shape, latency and amplitude of the ERP obtained by across-trial averaging in the time domain of simulated ERP data. The frequency distributions of single-trial latencies in the presence of different levels of jitter (positively skewed distribution with increasing variance from black to red) are shown in the insert. Note that, although the amplitude of single trial ERPs is the same in all three conditions, the asymmetrically distributed increase in latency jitter progressively distorts the original signal, leading to a reduction in peak amplitude, but also to an increase in peak latency of the waveform obtained by time-domain averaging. (For interpretation of the references to color in this figure legend, the reader is referred to the web version of this article.)

2.1.3. Spatial and temporal overlapping of multiple cortical generators

Although it is tempting to think that, given its high temporal resolution, EEG allows unravelling the time course of the different brain processes related to a particular event, the accurate interpretation of scalp responses is difficult because each scalp electrode records a spatially blurred mixture of neural activities. This spatial filtering is a consequence of volume conduction (i.e., the conduction of the signals through the anatomical structures interposed between the origin of the neural activity and the recording electrode). It is generally accepted that all but the earliest ERPs reflect activity arising from multiple, spatially distributed sources. Therefore, it is often difficult to disentangle (either in space or time) the different brain processes that may contribute to the signal recorded on the scalp.

3. Detecting electrical event-related brain responses: alternative methods

Because averaging in the time domain clearly makes a considerable part of the information present in single EEG epochs undetectable, a number of alternative signal-processing approaches have been suggested. Here, we will outline the principles underlying three different methods and focus on how the results obtained using these methods may be interpreted.

First, we will discuss methods relying on the joint decomposition of the EEG in both the time domain and the frequency domain. We will examine how these methods allow revealing ERPs affected by latency jitter, ERS and ERD. We will also show how these methods may allow distinguishing between ERPs and ERPRs.

Second, we will discuss methods that rely on independent component analysis (ICA) to perform a blind separation of EEG sources and examine how this may allow disentangling event-related brain responses that are temporally and spatially overlapped.

Third, we will discuss methods that have been proposed to analyse event-related brain responses at single-trial level (i.e., without resorting to across-trial averaging) and examine how this may disclose relevant physiological information.[3]

4. Detecting event-related EEG brain responses: time-frequency domain averaging

Several methods have been proposed to identify, characterize and quantify ERS and ERD [6]. All these different methods are based on techniques to estimate, within each single EEG epoch, the amplitude of oscillatory activity as a function of time and frequency. Because the estimate is a time- varying expression of oscillation amplitude *regardless of its phase*, averaging these estimates across trials discloses both phase-locked and non-phase-locked modulations of signal amplitude, provided that these modulations are both time locked to the onset of the event and consistent in frequency (i.e., the latency and frequency at which they occur are reproducible across trials).

In addition, some of these methods allow estimating the phase of the signal and therefore assess phase coherence across trials and channels (a parameter also known as 'phase-locking value' (PLV) or 'phase coherence').

4.1. Time-frequency decomposition of EEG epochs

A commonly used method consists in filtering EEG epochs within a given frequency band, squaring the filtered epochs and smoothing the resulting waveforms using a moving average of a predefined duration [15]. This method, although easy to implement, has one important drawback: the range of explored frequencies must be arbitrarily defined. Therefore, it is not well suited to exploring signals containing a wide range of frequencies (e.g., the EEG), especially because meaningful differences can be found in neighbouring EEG frequency bands [16]. Furthermore, the smoothing required to cancel out phase and thereby estimate the envelope of the signal results in a reduced temporal resolution.

[3] Most of these methods are implemented in two freely distributed software for the analysis of event-related EEG responses: LetsWave (http://amouraux.webnode.com/letswave) and EEGLAB (http://sccn.ucsd.edu/eeglab).

4.1.1. The windowed Fourier transform

The Fourier transform can be used to measure oscillation amplitude across the whole frequency spectrum. However, the Fourier transform contains no temporal information. To retain some temporal information, the Fourier transform can be performed on successive EEG segments defined by a windowing function ('short-term Fourier transform' or 'windowed Fourier transform'). This procedure expresses the amplitude and phase of the signal in both time and frequency. In analogy to Heisenberg's uncertainty principle, the width of the windowing function defines both the temporal and the frequency resolution of this method. The windowed Fourier transform uses a fixed and arbitrarily defined window width, thus resulting in a fixed time-frequency resolution. When defining a narrow window, temporal resolution will be high (i.e., it will be possible to resolve two events happening closely in time), but frequency resolution will be low (i.e., it will not be possible to resolve two events happening closely in frequency). On the opposite, when defining a wide window, the frequency resolution of the transform will be high, but at the cost of a low temporal resolution.

4.1.2. The continuous wavelet transform

By adapting the window width as a function of the estimated frequency, the continuous wavelet transform (CWT) offers an optimal compromise for time-frequency resolution and is therefore well suited to explore event-related modulations of the EEG spectrum in a wide range of frequencies. When estimating low frequencies, the CWT uses a wide window, resulting in low temporal resolution but high-frequency resolution. At these low frequencies, the loss of temporal resolution is irrelevant because the latencies of low frequency changes are uncertain by definition.[4] In contrast, when estimating high frequencies, the CWT uses a narrow window, resulting in high temporal resolution but low frequency resolution. At these high frequencies, the loss of frequency resolution is irrelevant because the frequencies composing short-lasting changes (e.g., a brief discontinuity in the signal) are uncertain by definition.

The Morlet function is the most often used family of wavelets, when applied to EEG data. It is a function of time t composed of a complex exponential modulated by a Gaussian envelope:

$$\psi(t) = \exp\left(-\frac{t^2}{2\sigma^2}\right)\exp\left(j\omega_0 t\right)$$

The Morlet has a Gaussian distribution in both the time and the frequency domain, centred around time t_0=0 and frequency ω_0. The spread of the Morlet function in time and frequency is defined by σ.

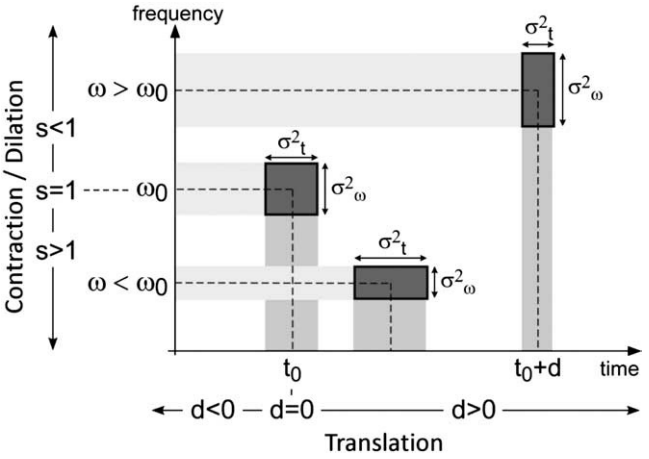

Fig. 4. Time-frequency decomposition of EEG data using the CWT (Morlet function). The Morlet function has a Gaussian distribution centred around time t_0 and frequency ω_0 Time and frequency variance of the function ($\sigma^2_{t,0}$ and $\sigma^2_{\omega,0}$) define the resolution of the decomposition. By translating the mother wavelet, parameter d defines the location in time of the daughter wavelet. By dilating and contracting the wavelet, parameter s not only defines the location in frequency of the daughter wavelet, but also the time/frequency resolution ratio. Note that the area represented by the product of both variances ($\sigma^2_{t,0}$, and $\sigma^2_{\omega,0}$) is constant. Adapted from Ref. [17].

This 'mother' function is then used to build a set of 'daughter' functions $\psi_{d,s}$ (t):

$$\psi_{d,s}(t) = \frac{1}{s}\psi\left(\frac{t-d}{s}\right)$$

By translating $\psi(t)$, the parameter d (or 'time-shift') defines the location in time of the daughter wavelet. By dilating or contracting $\psi(t)$, the parameter s (or 'scaling factor') adjusts not only the mean frequency of the wavelet, but also its spread. The variance of $\psi_{d,s}(t)$ in the time domain and in the frequency domain is thus not only a function of the variance of the mother wavelet, but also of s, the scaling factor. If the wavelet is dilated, the spread of the function is increased in the time domain while its spread in the frequency domain is proportionally reduced. On the contrary, if the wavelet is contracted, the spread of the function is decreased in the time domain while its spread in the frequency domain is proportionally increased. As time and frequency resolution of the wavelet transform are defined by the relative variance of the wavelet in time and frequency,[5] by adapting the window width as a function of the estimated frequency, CWT offers an optimal compromise for time-frequency resolution (Fig. 4).

The wavelet transform T_f (d,s) of $f(t)$ is the inner product of the wavelet function $\psi_{d,s}(t)$ with $f(t)$. The norm

[4] A typical example of this is the low-frequency drifts of the EEG signal.

[5] At one extreme of this relationship lies the Fourier transform applied to the whole signal. In that case, the frequency resolution of the transform is maximal, but contains no temporal information. At the other extreme of this relationship lies the untransformed signal. In that case, the temporal resolution is maximal, but contains no frequency information.

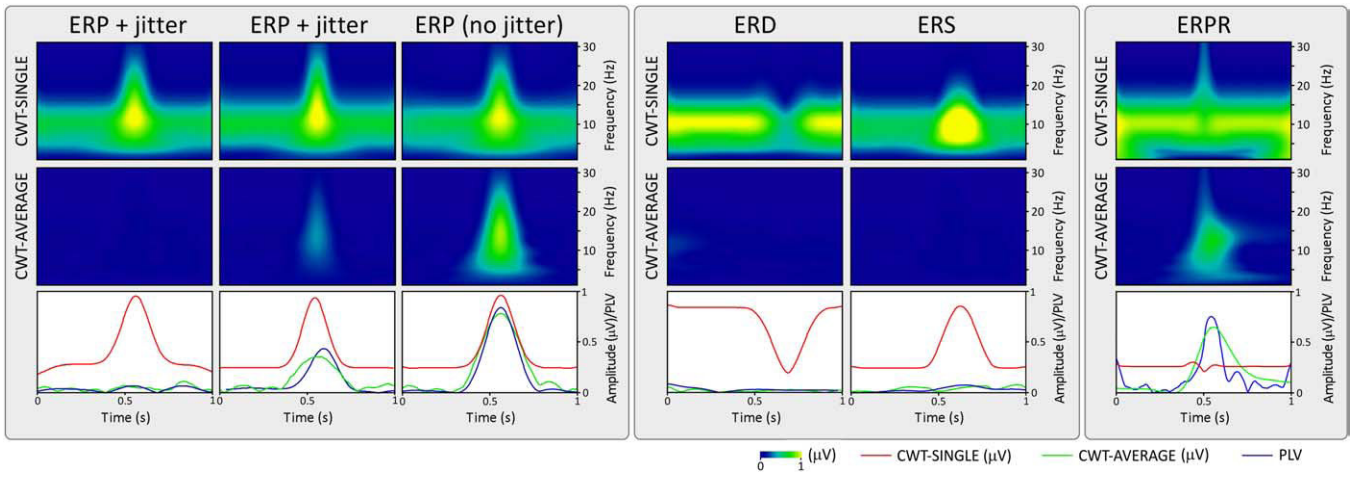

Fig. 5. Across-trial averaging of event-related electrical brain responses in the time-frequency domain. ERPs (left panel) were modelled as a time-locked deflection embedded in a background of non-phase-locked oscillations. ERD and ERS (middle panel) were modelled as a time-locked decrease/increase of background non-phase-locked oscillations. ERPR (right panel) was modelled as a time-locked resetting of the phase of ongoing, initially non-phase-locked oscillations (see also Fig. 1). *CWT-SINGLE.* A time-frequency representation of oscillation amplitude is obtained from each single epoch, and the obtained time-frequency matrices are subsequently averaged across trials. This procedure enhances the signal-to-noise ratio of both phase-locked and non-phase-locked electrical brain responses. Note the presence of a continuous activity centred around 10 Hz in all plots, corresponding to the modelled background oscillations. Note how CWT-SINGLE enhances ERPs (even when their latency is subject to a significant across-trial jitter), preserves the non-phase-locked oscillations (allowing revealing time-locked ERD and ERS), and how the discontinuity in the signal introduced by ERPR results in a transient redistribution of the signal amplitudes. *CWT-AVERAGE.* A time-frequency representation obtained from the waveform resulting from across-trials averaging in the time domain. Note how only ERPs devoid of latency jitter and ERPR are revealed by time-domain averaging. In the third row of the figure, amplitude values of 10-Hz oscillations obtained from CWT- SINGLE (red waveform) and CWT-AVERAGE (green waveform), and their PLV (a measure of phase locking across trials, blue waveform) are plotted against time. Note how PLV and CWT-AVERAGE follow the same trend, indicating that averaging in the time domain is able to preserve only phase-locked activities. (For interpretation of the references to color in this figure legend, the reader is referred to the web version of this article.)

of this complex value is an estimate of the oscillation amplitude of $f(t)$ around time and frequency defined by d and s. The argument is an estimate of its instantaneous phase. Time-frequency maps of oscillation amplitude or phase can thus be constructed using a set of daughter wavelets whose average frequency will range from the lowest to the highest frequency to be explored, and whose average latency will range from the lowest to the highest latency to be explored.

4.1.3. CWT of single EEG epochs (CWT-SINGLE)

To enhance the three possible event-related changes in the EEG signal that are time-locked, but not necessarily phase-locked to the eliciting event (i.e., non-phase-locked

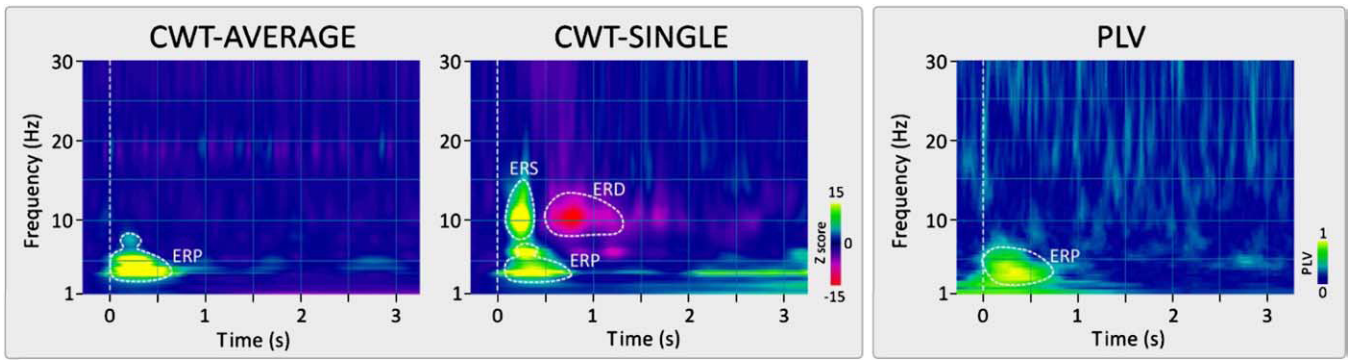

Fig. 6. Event-related brain responses revealed by decomposing signals in the time-frequency domain using the CWT (CWT-AVERAGE, CWT-SINGLE and PLV). Both CWT-AVERAGE and PLV reveal time-locked signal changes only when these signal changes are also phase-locked to the onset of the stimulus (i.e., ERPs and/or ERPR). In contrast, the CWT-SINGLE reveals time-locked signal changes whether or not phase-locked to the onset of the stimulus (i.e., ERPs with and without latency jitter, ERD and ERS). CWT-AVERAGE and CWT-SINGLE estimates of signal amplitude are expressed as Z scores, relative to a pre-stimulus reference interval (−0.4 to −0.1 s). The eliciting stimulus was a brief pulse of radiant heat (applied to the dorsum of the left hand) that elicited not only a series of event-related potentials (ERPs), but also at least two non-phase-locked responses of higher frequency (ERS and ERD). Note that the response labelled as 'ERS' could also be interpreted as an ERP rendered non-phase locked by a significant amount of latency jitter. Adapted from Ref. [17]. (This image may be viewed in color in the web version of this article.)

ERS and ERD, non-phase-locked ERPs subject to a significant latency jitter, and phase-locked ERPs), the CWT is applied to each single EEG epoch [17,18], prior to averaging across trials (CWT-SINGLE). Resulting time-frequency estimates are then used to compute a matrix expressing oscillation amplitude as a function of time and frequency. The average across trials of these matrices expresses the average EEG oscillation amplitude as a function of time (relative to stimulus onset) and frequency (Figs. 5 and 6). For each estimated frequency (i.e., each row of the matrix), the averaging procedure will preserve fluctuations in signal amplitude that occur at a fixed latency across trials, but smooth out fluctuations that are temporally unrelated to the stimulus onset. Thus, CWT-SINGLE enhances the signal-to-noise ratio of both phase-locked and non-phase-locked event-related EEG responses (Figs. 5 and 6).

4.1.4. CWT of EEG epochs averaged in the time domain (CWT-AVERAGE)

As outlined in Section 2, the standard average across trials of single EEG epochs enhances the signal-to-noise ratio of stimulus-related EEG changes that are phase-locked to the event onset (i.e., ERPs, phase resetting), but cancels out event-related EEG changes that are not phase locked (i.e., ERS and ERD). The CWT of EEG epochs averaged in the time domain (CWT-AVERAGE) can be computed to obtain a time-frequency representation of phase-locked EEG responses and thereby assess whether amplitude enhancements identified in the CWT-SINGLE transform correspond to phase-locked (ERPs) or non-phase-locked (ERS/ERD) activities (Figs. 5 and 6). Consequently, activities present in both the CWT-AVERAGE and the CWT-SINGLE should be considered as phase-locked (ERPs), while activities present only in the CWT-SINGLE should be considered as non phase-locked (ERD and ERS). Furthermore, activities present only in the CWT-AVERAGE may be hypothesized to reflect phase resetting (appearing as an increase of signal amplitude in the CWT-AVERAGE related to the fact that during the transient interval where these oscillations become phase-locked to the onset of the stimulus, they are not cancelled out by the averaging procedure).[6]

4.1.5. Phase-locking value

The PLV is a measure of how much phase locked (i.e., how stationary) the EEG signal is across trials. $\phi(d,s,n)$ is the estimated instantaneous phase of the n^{th} EEG epoch at time and frequency locations defined by d and s [9,19]. $PLV(d,s)$ is obtained by taking the norm of the average of $\phi(d,s,n)$ across N trials:

$$\mathrm{PLV}(d,s) = \frac{\left|\sum_{n=1}^{N} \phi(d,s,n)\right|}{N}$$

Consequently, PLV is a real value ranging between 0 (random phase across trials) and 1 (constant phase across trials). Therefore, if at a particular latency and frequency, the signal is mainly constituted by a response phase locked to the onset of the stimulus (i.e., an ERP) PLV will tend towards 1. On the contrary, if at that latency and frequency the signal amplitude is mainly constituted of EEG oscillations whose phase is unrelated to the stimulus, PLV will tend towards 0 (Figs. 5 and 6). It is important to note that, even though the PLV is obtained solely from an estimation of signal phase (and not signal amplitude), it may still be strongly influenced by the ratio between the amplitude of the explored EEG response and the amplitude of the background EEG activity. Indeed, if the signal-to-noise ratio of a perfectly phase-locked ERP is low, the PLV will be small (because the estimated instantaneous phase will mostly reflect that of the background, non-phase-locked activity). On the contrary, if the signal-to-noise ratio of that ERP is high, the PLV will be large (because the estimated instantaneous phase will mostly reflect that of the ERP). Therefore, when interpreting the difference between the PLV obtained in two experimental conditions, it is imperative to ascertain that the observed difference is not simply the result of a difference in the relative signal-to-noise ratio between phase-locked and non-phase-locked activities.

4.1.6. Phase-locking value between two scalp electrodes

In recent years, a lot of effort has been devoted to the investigation of how activities from cortical areas distributed over the brain may integrate and interact [9,20]. The possibility that such large-scale interactions could be mediated by neuronal assemblies oscillating in the gamma range has been proposed [8]. The formation of these transient assemblies would be achieved by neuronal activity oscillating in a phase-locked manner. For all these reasons, it is relevant to quantify the degree of phase locking of EEG oscillations recorded at different scalp locations. To measure how strongly the EEG signal recorded at a given scalp electrode is phase locked to the EEG signal recorded at another scalp electrode, the PLV across trials can be computed using the estimated phase difference between both signals. The obtained value ranges from 0 (random phase difference across trials) to 1 (constant phase difference across trials). However, the interpretation of PLV across channels is often problematic. Indeed, scalp electrodes integrate neural activities over large volumes. When the volumes recorded by two electrodes overlap, the shared neuronal population will create spurious synchrony between the signals. In other words, it is often impossible to

[6] However, it is necessary to mention that the situation is usually more complex than in this ideal example, for a number of reasons: (1) any change of phase entails a transient redistribution of its frequency; hence, even if pure phase resetting occurs, the CWT-SINGLE will always show a variation in amplitude; (2) phase resetting and actual increase of signal amplitude can occur concomitantly, thus making it difficult to disentangle the two possible contributions.

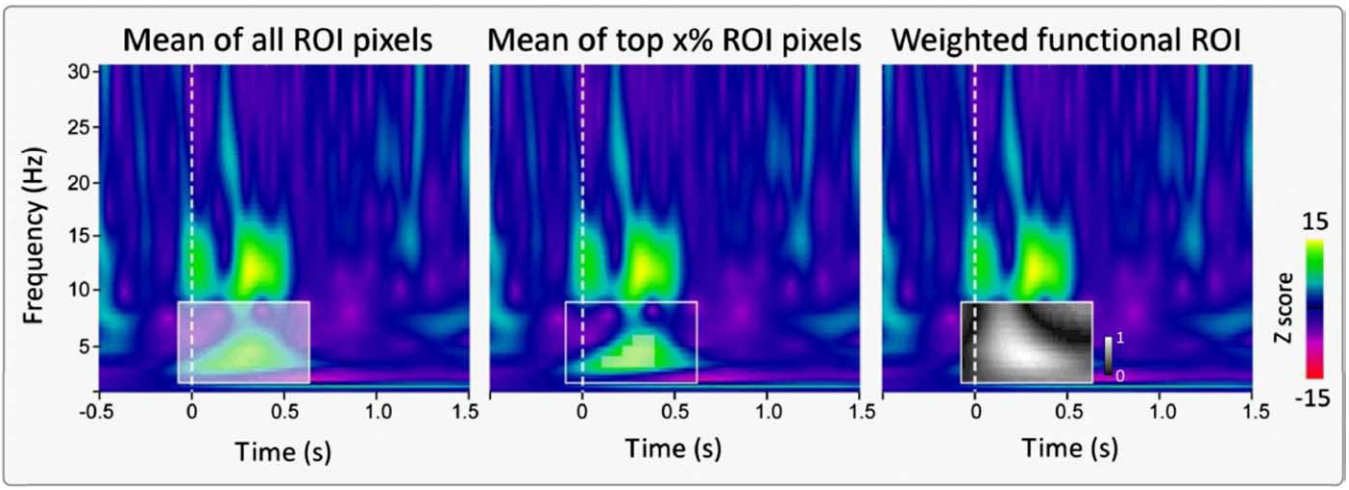

Fig. 7. Different methods for obtaining a summary value of the activity within a region of interest (ROI). *Mean of all ROI pixels*. This method simply consists in calculating the mean of all pixels enclosed within the ROI. Note how this method may miss a fraction of the response lying outside the ROI, but also how unrelated noise may contribute to the mean value. *Mean of top×% ROI pixels*. This method consists in calculating the mean of a predefined percentage of pixels having either the highest or the lowest values. By reducing the contribution of unrelated noise to the mean, this method allows defining a large ROI and thereby takes into account variability between subjects and between conditions while avoiding the problem of selecting just outlier values. *Weighted functional ROI*. A template of the time-frequency distribution of the response of interest is acquired in a separate recording session, specifically designed for that purpose. The response template is then used to build a weighted time-frequency mask (weights displayed as a grayscale) which will be used as ROI. (This image may be viewed in color in the web version of this article.)

distinguish clearly between an across-channel increase in PLV related to a true synchronization of two distinct sources and an across-channel increase in PLV simply resulting from volume conduction.

4.1.7. Looking for differences between experimental conditions

4.1.7.1. Expressing changes relative to baseline. ERS and ERD are usually expressed as a percentage of change relative to the average amplitude of a reference interval (ERS%, ERD %) [15], or, to take into account the variance of amplitude within that reference interval, they can be also expressed as deviations from the mean (*Z*-score) [17]. Whatever the criterion to express differences, the procedure is performed separately for each estimated frequency (i.e., each row in the time-frequency matrix). When defining the interval to be used as reference, it is important to take into account the fact that at lower frequencies the wavelet function is very spread in the time domain. For this reason, to reduce the influence of oscillations occurring after the onset of the event on the reference interval, the time points closely preceding the onset of the event should not be included in the reference interval.

4.1.7.2. Region of interests. When comparing the time-frequency matrices across different experimental conditions, regions of interest (ROIs) in the time-frequency matrix are often employed to reduce the number of comparisons. The boundaries of the ROI can be either (1) arbitrarily defined or (2) functionally defined using a method similar to the functional localizer used in functional magnetic resonance imaging (fMRI) [21]. In the latter case, a template of the electrophysiological pattern of interest is defined using the results obtained in a separate recording session, specifically designed for that purpose. This response template is then used to build a weighted time-frequency filter or mask which will be used as ROI (Fig. 7, right panel).

Whatever the procedure of defining the ROI, two methods of summarizing its activity can be used.

A simple method is to average all the time-frequency pixels the ROI contains (Fig. 7, left panel) [17]. This method has one main disadvantage: if the ROI is too strictly defined, the obtained summary value will miss the fraction of the response lying outside the ROI.[7] On the contrary, if the ROI is too loosely defined, unrelated noise included in the ROI will make it less effective at detecting significant differences across conditions.

An alternative method ('top x% approach' [22,23]) consists in selecting a predefined percentage of pixels having either the highest amplitude values (defining an ERS or an ERP) or the lowest amplitude values (defining an ERD) (Fig. 7, right panel). This approach, because it allows defining a large ROI, presents several advantages: (1) it takes into account the functional variability between subjects, (2) it avoids the problem of selecting just outlier values, (3) it allows comparing the same number of pixels for each ROI across experimental conditions, and (4) it reduces the

[7] Because of the important between-subject variability, this is especially true when comparing results across subjects.

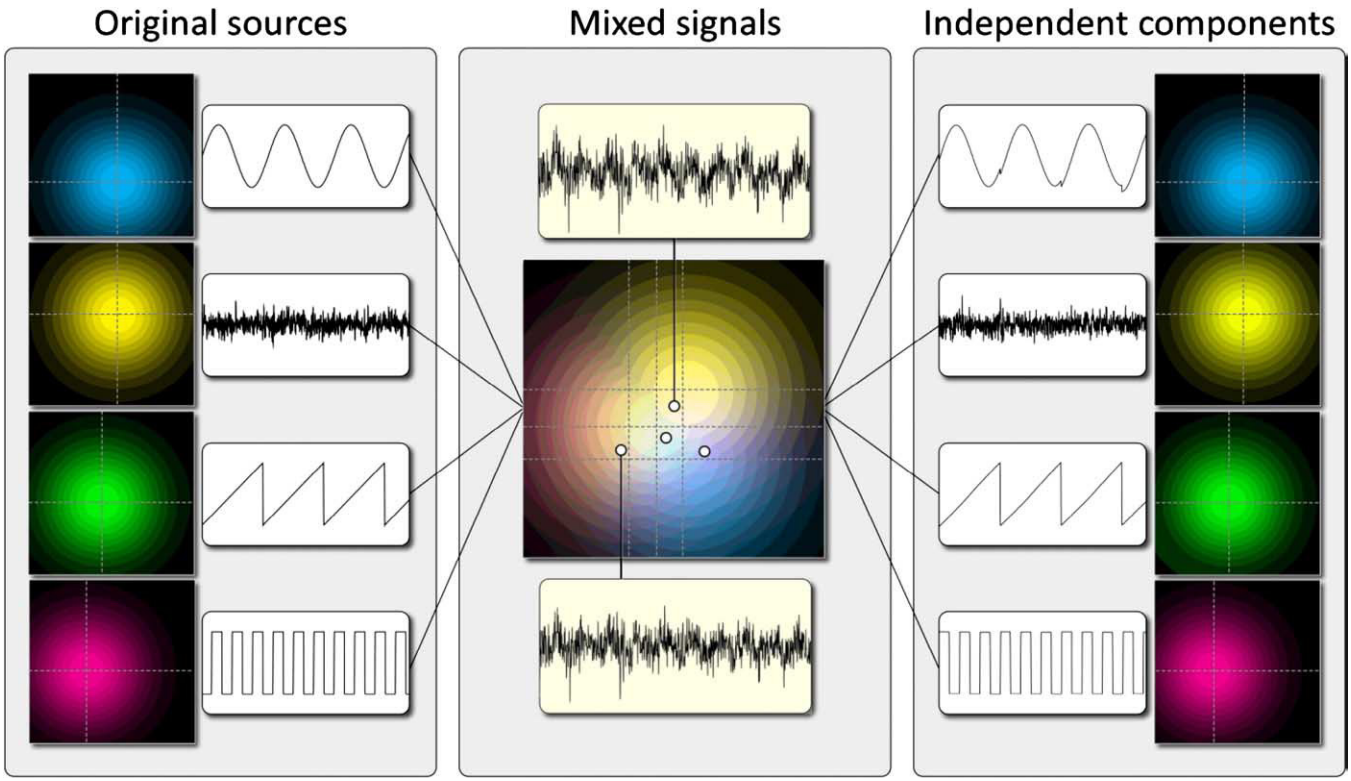

Fig. 8. Blind source separation of simulated data using an Independent Component Analysis (ICA). Four sources (left panel) having independent time courses (shown in the insets) were projected onto a two-dimensional plane using strongly overlapping yet distinct Gaussian spatial distributions. The colored maps represent the strength of the projection onto the plane. The linear mixture of these temporally-independent spatially-overlapping sources are shown in the middle panel (waveforms represent the mixed signals at two distinct points of the plane). A sample of this mixture of signals (four locations shown as small white disks) was then separated using an ICA (runica [24,25]). The time course and spatial distribution of the obtained independent components are shown in the right panel. Note how the blind source separation algorithm was able to resolve accurately the time course and spatial distribution of the original sources contributing to the mixed signals. (For interpretation of the references to color in this figure legend, the reader is referred to the web version of this article.)

'regression to the mean' problem, which can significantly bias the experimental results [23].

5. Spatio-temporal decomposition of event-related brain responses

Due to volume conduction (i.e., the conduction of the electric current source through the anatomical structures interposed between the neural sources and the recording electrodes), scalp potentials are spatially blurred. Given the physical properties of the volume conductor [1], it is reasonable to model the EEG recorded by each scalp electrode as a linear mixture of all the contributing underlying sources of electrical activity, some of which may be of cortical origin and some of which may not (e.g., eye movement, muscle, or cardiac-related artefacts). For this reason, it is generally accepted that most event-related EEG responses recorded on the scalp reflect the activity of several, spatially smeared, temporally overlapping, yet functionally and spatially distinct sources of brain activity.[8] Although often difficult, disentangling these mixed sources of activity is important to achieve a correct functional interpretation of the recorded brain responses.

Blind source separation algorithms (Fig. 8) are used in signal processing to recover independent sources (e.g., the voices of different people talking simultaneously in a room) from signals obtained from sensors that record a linear mixture of these sources (e.g., microphones positioned at different locations in that room). Therefore, these algorithms are very well suited for the analysis of scalp EEG. Independent component analysis has been used successfully by a growing number of investigators to perform blind source separation of scalp EEG [24,26]. When applied to multi-channel recordings, the goal of ICA is to unmix signals recorded on the scalp into a single linear combination of independent components (ICs), each having a maximally independent time course and a fixed scalp distribution.[9]

[8] One exception to this case is the early ERPs elicited by sensory stimuli (e.g., the N20 deflection in response to electrical stimulation of the median nerve), which are thought to reflect the activity of a single source, corresponding to the initial response occurring in primary sensory cortices.

[9] Multi-channel scalp potentials recorded at n different time points and at p different scalp sensors may be written as X, a matrix having p rows and n columns. ICA optimizes an unmixing matrix W which linearly unmixes X into $U=WX$, a matrix containing p maximally independent time courses. Each of these time courses has a fixed scalp distribution, characterized by the corresponding column of the inverse matrix W^{-1}, containing the relative projection of the component onto the different scalp sensors.

Applied to non-averaged multi-channel EEG recordings, the method has proven very efficient at isolating and removing non-neural artifacts that affect the recorded EEG [27,28]. Applied to EEG epochs averaged in the time domain (Fig. 9) and, more recently, applied to non-averaged concatenated EEG epochs, ICA has allowed separating late cognitive ERPs into distinct, independent constituents [24,26].

An IC does not necessarily represent an anatomically discrete source of activity. Indeed, an IC is defined by its temporal independence relative to the other sources of activity. If the activities within two distinct regions of the brain strongly covary, they will be represented within a single component.

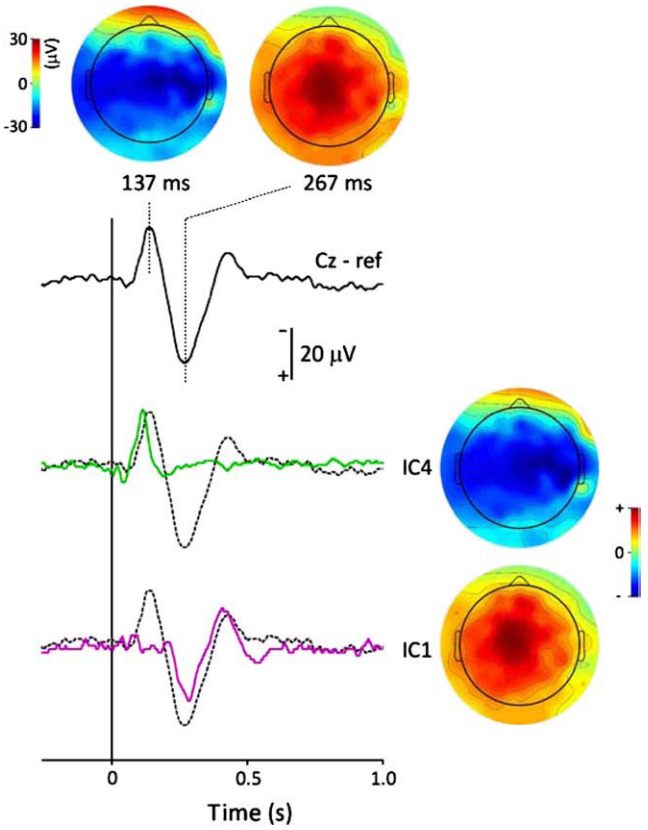

Fig. 9. Blind source separation of ERPs using probabilistic ICA [24,29]. Late somatosensory ERPs were elicited by the electrical stimulation of the right *nervus radialis superficialis* and recorded using 124 scalp electrodes. The top waveform shows the average across trials in the time domain (Cz-nose reference). The bulk of the signal consisted in a negative deflection peaking at 137 ms, followed by a positive deflection peaking at 267 ms. The scalp distribution of both peaks is shown in the upper scalp maps. To constrain ICA, an objective estimate of dimensionality was obtained using a method based on maximum likelihoods and operating on the *eigenvalues* of principal component analysis [29,30]. The estimated number of dimensions was 16. The time course of two independent components contributing respectively to the negative deflection (IC4: green waveform) and the positive deflection (IC1: purple waveform) is shown in the lower graphs, along with their corresponding scalp distributions. Note how the blind source separation algorithm was able to effectively separate both peaks into distinct components. (For interpretation of the references to color in this figure legend, the reader is referred to the web version of this article.)

When ICA is unconstrained, the total number of estimated ICs equals the total number of recording electrodes. If that number is considerably greater than the true number of independent sources contributing to the recorded signals, ICs containing spurious activity will appear because of overfitting. On the opposite, if the total number of ICs is considerably smaller than the true number of underlying sources, valuable information will be lost because of underfitting. This important limitation (that the number of independent components is arbitrarily defined) could explain why, until now, ICA has not been able to clearly and unequivocally disentangle event-related electrical brain responses into physiologically meaningful independent constituents.[10]

Constraining ICA to a number of dimensions that is based on an effective estimate of the intrinsic dimensionality of the original data may provide a solution to this critical problem [29]. This approach, called probabilistic ICA, has been successfully applied to the analysis of fMRI data. Because the risk of overfitting or underfitting the data is reduced, each obtained IC is much more likely to reflect a single physical or physiological source of activity.

6. Measuring electrical brain responses to transient events without averaging

As detailed in Section 2, across-trial averaging of EEG epochs is often a necessary step to obtain a reliable estimate of event-related brain responses. However, the cost of this procedure is that all the information concerning the across-trial variability of these responses is lost. Several methods have been proposed to denoise and estimate certain characteristics of event-related electrical brain responses at the level of single trial. By allowing a direct exploration of the dynamics between different features of electrical brain responses (e.g., the peak latency and amplitude of a given ERP), behavioural variables (e.g., the intensity of perception, the reaction-time latency) [31] and also features of brain responses sampled using different neuroimaging modalities (e.g., fMRI) [32,33], these methods may provide new insights into the functional significance of the different brain processes that underlie these brain responses. Indeed, across-trial variability may reflect important experimental factors such as modulations of peripheral sensory input [31,34], or changes in subject performance related to fluctuations in vigilance, expectation, attentional focus or task strategy [35]. Furthermore, as shown in Section 2.1, across-trial variability of electrical brain responses, and latency jitter in particular, can significantly distort the

[10] An additional problem is that, when the study involves the recording of electrical brain responses in multiple subjects or in multiple sessions, a method to determine which ICs are common across subjects or sessions is needed. To achieve this, methods for clustering ICs have been developed, based, for example, on the components scalp projections, or their spectrum of activity [27].

average ERP and thereby lead to misestimating its amplitude and latency.

6.1. Manual measurement of single-trial ERPs

A simple way to obtain single-trial ERP information consists in attempting to visually identify and measure, within each single EEG epoch, a given event-related peak of activity. This approach has been shown to be reasonably effective for ERPs that have particularly large amplitudes [31,36].

However, because the signal-to-noise ratio is generally low, this approach is often impracticable. If it is nevertheless attempted, the estimate is likely to reflect the spurious detection of uncorrelated noise resembling the searched-for visual template. Although the task can be assigned to an independent observer, the method remains prone to the introduction of biases, and the obtained results are difficult to replicate. Furthermore, because the observer attempts to best fit the projected response within a noise-embedded signal, the method almost inevitably leads to an overestimation of response amplitude.

6.2. Automatic single-trial measurement of ERPs using a multiple linear regression

Recently, we showed that a multiple linear regression approach can be used to obtain an unbiased and accurate estimate of latency and amplitude of single-trial ERPs (Fig. 10) [37]. This method has been successfully applied to late somatosensory and auditory ERPs [33,34,38]. In principle, it could also be applied to the time-frequency decompositions of single EEG epochs and thereby be used to estimate non-phase-locked brain responses (ERS and ERD). In this method, a basis set of regressors and their temporal derivatives are obtained from the across-trial average waveform. This basis set is then regressed against each single EEG epoch, thus providing a quantitative measure of peak latency and amplitude of the different ERP waves present in each single epoch. The inclusion of temporal derivatives allows modelling the temporal variability of the responses and provides an estimate of single-trial wave latencies. Furthermore, as the method allows the amplitude of each single-trial response to be positive or negative, the effect of uncorrelated peaks in the signal, due to background activity, is treated without bias. Therefore, if a sufficient number of trials are considered, the contribution of non-event-related peaks will tend towards zero.

6.3. Denoising single-trial EEG epochs using spatial filters

In Section 5 we showed that blind source separation algorithms, and in particular ICA, could be used to separate linear mixtures of signals into their independent constituents. Jung et al. [27] showed that the obtained spatial filters may be used to separate efficiently ERPs from artifacts related to eye movements, eye blinks and muscle activity, but also from the background EEG activity. The result is a marked increase in signal-to-noise ratio allowing a more robust single-trial estimate of ERPs [39,40].

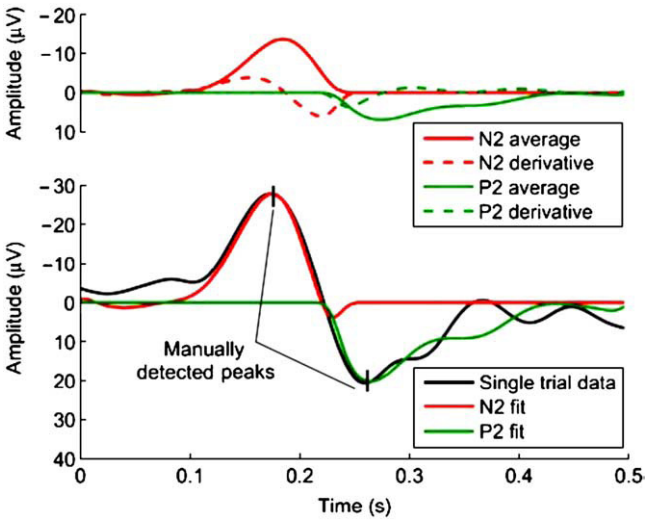

Fig. 10. Automatic single-trial measurement of ERPs using multiple linear regression. Upper panel: Four regressors were obtained from the average in the time domain of the event-related brain potentials elicited by brief infrared laser pulses (activating Aδ-fibre skin nociceptors) applied to the dorsum of the right hand and recorded from the vertex (Cz-nose reference). The solid waveforms represent the negative (N2, in red) and positive (P2, in green) deflections of the average in the time domain, and the dashed waveforms represent their corresponding temporal derivatives. Lower panel: The multiple linear regression of these four basis vectors against each single EEG epoch was used to model each single-trial ERP. The black waveform corresponds to a single representative trial. The red and green waveforms correspond to the automated fittings of the N2 and P2 deflections, respectively. The vertical lines correspond to the latency of the N2 and P2 peaks detected by an independent observer. Modified from Ref. [37]. (For interpretation of the references to color in this figure legend, the reader is referred to the web version of this article.)

6.4. Denoising single-trial EEG epochs with time-frequency filters

In Section 4 we showed that time-frequency decomposition methods, such as the wavelet transform, can separate signals in the frequency domain, while preserving a significant amount of temporal information. The frequency distribution of at least a fraction of uncorrelated background EEG activity and non-brain artefacts differs from that of event-related electrical brain responses. Therefore, to attenuate the contribution of activities unrelated to the event, the joint time-frequency decomposition of EEG epochs can be used to apply a time-varying frequency filter, optimally adjusted to the time-varying frequency distribution of event-related brain responses. This procedure efficiently enhances the signal-to-noise ratio of single EEG epochs [41,42]. The fact that time-frequency approaches produce a single-trial estimate that accounts for both phase-locked and non-phase-locked event-related responses also contributes to the efficiency of this denoising approach.

Acknowledgments

Andre Mouraux is Marie-Curie post-doctoral Research Fellow and Chargé de recherches of the Belgian National Fund for Scientific Research (FNRS). Giandomenico Iannetti is University Research Fellow of The Royal Society.

References

[1] Nunez P, Srinivasan R. Electric fields of the brain. The neurophysics of EEG. 2nd ed. Oxford University Press; 2006.
[2] Luck SJ. An Introduction to the Event-Related Potential Technique. Cambridge: MIT Press; 2005.
[3] Pfurtscheller G, Cooper R. Frequency dependence of the transmission of the EEG from cortex to scalp. Electroencephalogr Clin Neurophysiol 1975;38(1):93–6.
[4] Baker SN, Curio G, Lemon RN. EEG oscillations at 600 Hz are macroscopic markers for cortical spike bursts. J Physiol 2003;550(Pt 2):529–34.
[5] Berger H. Über das elektroenkephalogramm des menschen. Arch Psychiatry 1929(87):527–70.
[6] Pfurtscheller G, Lopes da Silva FH. Event-related EEG/MEG synchronization and desynchronization: basic principles. Clin Neurophysiol 1999;110(11):1842–57.
[7] Pfurtscheller G, Neuper C. Event-related synchronization of mu rhythm in the EEG over the cortical hand area in man. Neurosci Lett 1994;174(1):93–6.
[8] Singer W. Synchronization of cortical activity and its putative role in information processing and learning. Annu Rev Physiol 1993;55:349–74.
[9] Rodriguez E, George N, Lachaux JP, Martinerie J, Renault B, Varela FJ. Perception's shadow: long-distance synchronization of human brain activity. Nature 1999;397(6718):430–3.
[10] Sauseng P, Klimesch W, Gruber WR, Hanslmayr S, Freunberger R, Doppelmayr M. Are event- related potential components generated by phase resetting of brain oscillations? A critical discussion. Neuroscience 2007;146(4):1435–44.
[11] Tass PA. Phase Resetting in Medicine and Biology. 2nd ed. Springer; 2006.
[12] Dawson GD. A summation technique for detecting small signals in a large irregular background. J Physiol 1951;115(1):2p–3p.
[13] Dawson GD. A summation technique for the detection of small evoked potentials. Electroencephalogr Clin Neurophysiol 1954;6(1):65–84.
[14] Srinivasan R. High-resolution EEG: theory and practice. In: Handy T, editor. Event-related potentials: a methods handbook. Cambridge: The MIT Press; 2005. p. 167–88.
[15] Pfurtscheller G, Lopes da Silva FH. Event-related EEG/MEG synchronization and desynchronization: basic principles. Clin Neurophysiol 1999;110(11):1842–57.
[16] Pfurtscheller G, Klimesch W. Functional topography during a visuoverbal judgment task studied with event-related desynchronization mapping. J Clin Neurophysiol 1992;9(1):120–31.
[17] Mouraux A, Guerit JM, Plaghki L. Non-phase locked electroencephalogram (EEG) responses to CO_2 laser skin stimulations may reflect central interactions between A partial differential- and C-fibre afferent volleys. Clin Neurophysiol 2003;114(4):710–22.
[18] Tallon-Baudry C, Bertrand O, Delpuech C, Permier J. Oscillatory gamma-band (30–70 Hz) activity induced by a visual search task in humans. J Neurosci 1997;17(2):722–34.
[19] Lachaux JP, Rodriguez E, Martinerie J, Varela FJ. Measuring phase synchrony in brain signals. Hum Brain Mapp 1999;8(4):194–208.
[20] Lachaux JP, Rodriguez E, Martinerie J, Adam C, Hasboun D, Varela FJ. A quantitative study of gamma-band activity in human intracranial recordings triggered by visual stimuli. Eur J Neurosci 2000;12(7):2608–22.
[21] Mouraux A, Plaghki L. Single-trial detection of human brain responses evoked by laser activation of Adelta-nociceptors using the wavelet transform of EEG epochs. Neurosci Lett 2004;361(1–3):241–4.
[22] Iannetti GD, Zambreanu L, Wise RG, Buchanan TJ, Huggins JP, Smart TS, et al. Pharmacological modulation of pain-related brain activity during normal and central sensitization states in humans. Proc Natl Acad Sci U S A 2005;102(50):18195–200.
[23] Mitsis GD, Iannetti GD, Smart T, Tracey I, Wise RG. Regions of interest analysis in pharmacological fMRI: how do the definition criteria influence the inferred result? Neuroimage 2008;40(1):121–32.
[24] Makeig S, Jung TP, Bell AJ, Ghahremani D, Sejnowski TJ. Blind separation of auditory event-related brain responses into independent components. Proc Natl Acad Sci U S A 1997;94(20):10979–84.
[25] Bell AJ, Sejnowski TJ. An information-maximization approach to blind separation and blind deconvolution. Neural Comput 1995;7(6):1129–59.
[26] Makeig S, Debener S, Onton J, Delorme A. Mining event-related brain dynamics. Trends Cogn Sci 2004;8(5):204–10.
[27] Jung TP, Makeig S, Westerfield M, Townsend J, Courchesne E, Sejnowski TJ. Removal of eye activity artifacts from visual event-related potentials in normal and clinical subjects. Clin Neurophysiol 2000;111(10):1745–58.
[28] Makeig S, Enghoff S, Jung TP, Sejnowski TJ. Moving-window ICA decomposition of EEG data reveals event-related changes in oscillatory brain activity. 2nd Int. Workshop on Independent Component Analysis and Signal Separation; 2000. p. 627–32.
[29] Beckmann CF, Smith SM. Probabilistic independent component analysis for functional magnetic resonance imaging. IEEE Trans Med Imaging 2004;23(2):137–52.
[30] Rajan JJ, Rayner PJW. Model order selection for the singular value decomposition and the discrete Karhunen–Loeve transform using a Bayesian approach. Vision, Image Signal Proc IEE Proc 1997;144(2):116–23.
[31] Iannetti GD, Zambreanu L, Cruccu G, Tracey I. Operculoinsular cortex encodes pain intensity at the earliest stages of cortical processing as indicated by amplitude of laser-evoked potentials in humans. Neuroscience 2005;131(1):199–208.
[32] Mayhew S, Dirckx S, Niazy R, Iannetti G, Wise R. Habituation of the visual evoked potential (VEP) amplitude is not reflected in simultaneously acquired fMRI BOLD signal increase. in 13th Annual Meeting Human Brain Mapping; 2007, Chicago.
[33] Mayhew SD, Dirckx SG, Niazy RKN, Iannetti GD, Wise RG. Auditory-evoked scalp potentials may be recorded simultaneously with continuous fMRI scanning. in 13th Annual Meeting Human Brain Mapping; 2007, Chicago.
[34] Iannetti GD, Zambreanu L, Tracey I. Similar nociceptive afferents mediate psychophysical and electrophysiological responses to heat stimulation of glabrous and hairy skin in humans. J Physiol 2006;577(Pt 1):235–48.
[35] Haig AR, Gordon E, Rogers G, Anderson J. Classification of single-trial ERP sub-types: application of globally optimal vector quantization using simulated annealing. Electroencephalogr Clin Neurophysiol 1995;94(4):288–97.
[36] Purves AM, Boyd SG. Time-shifted averaging for laser evoked potentials. Electroencephalogr Clin Neurophysiol 1993;88(2):118–22.
[37] Mayhew SD, Iannetti GD, Woolrich MW, Wise RG. Automated single-trial measurement of amplitude and latency of laser-evoked potentials (LEPs) using multiple linear regression. Clin Neurophysiol 2006;117(6):1331–44.
[38] Wise RG, Iannetti GD, Mayhew SD, Rogers R, Pattinson KT, Tracey I. Assessment of opioid- induced analgesia and hyperalgesia using laser-evoked potentials. in 12th Annual Meeting Human Brain Mapping; 2006, Florence.

[39] Jung TP, Makeig S, Westerfield M, Townsend J, Courchesne E, Sejnowski TJ. Analysis and visualization of single-trial event-related potentials. Hum Brain Mapp 2001;14(3):166–85.

[40] Zouridakis G, Iyer D, Diaz J, Patidar U. Estimation of individual evoked potential components using iterative independent component analysis. Phys Med Biol 2007;52(17):5353–68.

[41] Mouraux A, Plaghki L. Single-trial detection of human brain responses evoked by laser activation of Adelta-nociceptors using the wavelet transform of EEG epochs. Neurosci Lett 2004;361(1–3): 241–4.

[42] Quian Quiroga R, Garcia H. Single-trial event-related potentials with wavelet denoising. Clin Neurophysiol 2003;114(2):376–90.